SPANDIDOS PUBLICATIONS

INTERNATIONAL JOURNAL OF ONCOLOGY 55: 1385-1395, 2019

Upregulated expression of eIF3C is associated with malignant behavior in renal cell carcinoma

MIN FAN*, KAI WANG*, XIAOHUI WEI, HONGWEI YAO, ZHEN CHEN and XIAOZHOU HE

Department of Urology, The Third Affiliated Hospital of Soochow University, Changzhou, Jiangsu 213003, P.R. China

Received January 29, 2019; Accepted October 1, 2019

DOI: 10.3892/ijo.2019.4903

Abstract. Eukaryotic initiation factor 3c (eIF3C) is involved in the initiation of protein translation. Aberrant eIF3C expression has been reported in different types of human cancer. The present study aimed to assess the role of eIF3C in the malignant behavior of renal cell carcinoma *in vitro* and *in vivo*. eIF3C expression was assessed in 16 pairs of renal cell carcinoma (RCC) and matched distant normal tissues, and in RCC cell lines using immunohistochemistry. Subsequently, eIF3C was depleted using lentiviral short hairpin RNA and cell proliferation, cell cycle distribution and apoptosis of these eIF3C-depleted cells were examined. Additionally, tumor cell xenograft assays in nude mice, Affymetrix microarrays and ingenuity pathway analyses were performed. eIF3C expression was upregulated in RCC tissues and cell lines. Depletion of eIF3C reduced tumor cell proliferation and arrested them at the G_1 stage, thus promoting their apoptosis *in vitro*. Depletion of eIF3C also inhibited the formation and growth of tumor cell xenografts in nude mice. In addition, depletion of eIF3C altered the expression levels of 994 differentially expressed genes in RCC cells (516 genes were upregulated and 478 genes were downregulated). The expression levels of phosphorylated-AKT, c-JUN and NFKB inhibitor α were lower in the shorth hairpin RNA eIF3C-transfected RCC cells compared with in the control group. In conclusion, the present study demonstrated that upregulated eIF3C expression contributed to the development and progression of RCC. Future studies should further evaluate whether eIF3C could be used as a potential strategy for RCC targeting therapy.

Correspondence to: Dr Xiaozhou He or Mr. Zhen Chen, Department of Urology, The Third Affiliated Hospital of Soochow University, 185 Juqian Street, Changzhou, Jiangsu 213003, P.R. China
E-mail: xiaozhouhe123@163.com
E-mail: chenzhen168@126.com

*Contributed equally

Abbreviations: eIFs, eukaryotic initiation factors; eIF3C, eukaryotic initiation factor 3c; RCC, renal cell carcinoma; DAB, 3,3'-diaminobenzidine; GFP, green fluorescence protein; RT-qPCR, reverse transcription-quantitative polymerase chain reaction

Key words: renal cell carcinoma, eukaryotic initiation factor 3c, cell cycle arrest, apoptosis, proliferation

Introduction

There are >200,000 newly-diagnosed cases of kidney cancer each year globally according to a statistic calculated in 2013, with the highest incidence in North America and the lowest incidence in Asia and Africa (1). Histologically, kidney cancer can be divided into two common types: Renal cell carcinoma (RCC) and transitional cell carcinoma (2). RCC is the most common type of kidney cancer, accounting for 90-95% of cases in adults (3). The incidence and mortality of kidney cancer have also increased over the past decades at a rate of 2-3% per decade (3). Generally, RCC is asymptomatic, and is, therefore, frequently diagnosed at an advanced stage (4), and up to 30% of patients with RCC exhibit a metastatic tumor at diagnosis (3). To date, surgery remains the most effective treatment for RCC, whereas it is usually resistant to conventional chemoradiotherapy (5). Therefore, an improved understanding of the biology of RCC can help us develop novel therapeutic strategies and identify biomarkers for early detection and prediction of prognosis and treatment responses, leading to enhanced effectiveness of RCC control in clinical practice.

Previous studies have revealed that RCC development is associated with gene mutations in chromosome 3p, which activate oncogenes, such as c-Met, or inactivate tumor suppressor genes, such as VHL (6,7). However, alterations of various genes and gene pathways have also been associated with the development and progression of RCC (8-12). The present study of the gene alterations in RCC focused on eukaryotic initiation factors (eIFs). Aberrant expression levels of eIFs have been observed in several types of human cancer (13). eIFs regulate the initiation of protein translation in eukaryotic cells (14). For example, eIF3, the largest initiation factor, binds to the 40S ribosomal subunit, different initiation factors and mRNA to facilitate protein translation in cells (15,16). Overexpression or underexpression of a particular eIF3 subunit is associated with the development and progression of a number of tumors, including lung cancer, breast cancer, hepatocellular cancer and intestinal cancer (17). During carcinogenesis and tumor progression, gene transcription and protein translation are usually upregulated in tumor cells (18). This has been confirmed in various previous studies of eukaryotic

initiation factor 3c (eIF3C) in testicular seminoma (19), meningiomas (20), glioma (21,22), colorectal cancer (22), hepatocellular carcinoma (24,25) and breast cancer (26). Nevertheless, to the best of our knowledge, the role of eIF3C in RCC has not been assessed.

In a preliminary experiment, the eIF3C mRNA level was higher in RCC tissue than in adjacent normal tissues (Fig. S1). Therefore, the present study aimed to evaluate whether eIF3C could be used as a potential diagnostic marker or therapeutic target for RCC. To address this, eIF3C expression was assessed in RCC and normal kidney tissues, and the role of eIF3C in RCC malignant behavior was examined *in vitro* and *in vivo*.

Materials and methods

Patients and tissue collection. A total of 16 pairs of tumor and matched distant normal tissues were collected from patients with RCC (11 men and 5 women; median age at diagnosis, 54 years; age range, 37-74 years) who underwent radical resection between February 2016 and July 2016 at the Third Affiliated Hospital of Soochow University. Distant normal tissues were obtained >5 cm away from tumors to ensure their normality. All patients were histologically diagnosed with RCC and did not receive any pre-surgery chemotherapy or radiotherapy. The present study was approved by the Ethics Committee of the Third Affiliated Hospital of Soochow University according to the principles of the Declaration of Helsinki. Written informed consent was provided by all participants prior to enrollment.

Immunohistochemistry. Tissues were fixed in 10% formalin at 4˚C for 10 h. Fixed and paraffin-embedded tissue blocks were retrieved from the Pathology Department of The Third Affiliated Hospital of Soochow University and cut into 4-μm thick sections. For immunostaining of the eIF3C protein, the sections were deparaffinized in xylene and rehydrated in descending alcohol series. Antigens were repaired by heating the tissue sections at 100˚C for 30 min in citrate (10 mmol/l; pH 6.0) (Beyotime). Then, the sections were immersed in a 0.3% hydrogen peroxide solution for 30 min to block endogenous peroxidase activity, rinsed in PBS for 5 min, blocked with 3% BSA (Beyotime Institute of Biotechnology) at room temperature for 30 min, and incubated with a primary antibody at 4˚C overnight according to the manufacturer's instructions. Subsequently, the sections were incubated with the secondary antibody at 37˚C for 30 min. The antigen-antibody complex was visualized after adding 3,3'-diaminobenzidine (DAB) for 2 min at room temperature. The primary antibody against eIF3C (1:1,000 dilution; cat. no. ab170841) was purchased from Abcam, and the secondary antibody and DAB were part of the MaxVision™ horseradish peroxidase (HRP)-Polymer anti-Mouse/Rabbit IHC kit (cat. no. 5010; Maxim Biotech, Inc.).

The immunostained sections were independently reviewed by two experienced pathologists who were blinded to the clinical parameters of the patients, and scores were evaluated from five randomly selected x20 microscopic fields under a light microscope (Olympus Corporation), according to a previously described H-score method (25). The H-score = (% unstained tumor cells x0) + (% weakly stained tumor cells x1) + (% moderately stained tumor cells x2) + (% strongly stained tumor cells x3). The H-scores ranged between 0 (100% negative staining) and 300 (100% strong staining).

Cell lines and culture conditions. Four human RCC lines ACHN, 786-O, Caki-1 and A498, were obtained from The Cell Bank of Type Culture Collection of the Chinese Academy of Sciences in September 2017 and maintained in RPMI-1640 medium (Invitrogen; Thermo Fisher Scientific, Inc.) supplemented with 10% fetal bovine serum (FBS; Biological Industries) and 1% penicillin-streptomycin (Invitrogen; Thermo Fisher Scientific, Inc.) at 37˚C in a humidified incubator with 5% CO_2. All cell lines were certified by Shanghai GeneChem Co., Ltd. for short tandem repeat analysis on October 31, 2017, as described in 2012 in American National Standards Institute Standard by the American Type Culture Collection Standards Development Organization (28) and in Capes-Davis *et al* (29). All cell lines were passaged <30 times.

Short hairpin RNA (shRNA) and cell transfection. Lentiviruses carrying eIF3C shRNA (cat. no. PSC2752) targeting the DNA sequence of 5'-GTCACTAAAGGTCTGTTTA-3', and negative control shRNA (cat. no. PSC3741) with a targeting sequence of 5'-TTCTCCGAACGTGTCACGT-3' were obtained from Shanghai GeneChem Co., Ltd. Both eIF3C and negative control shRNA were designed and cloned into the GV115 vector (Shanghai GeneChem Co., Ltd.) double enzyme digested by *Age*I/*Eco*RI. Reconstructed vectors with eIF3C-shRNA and the negative control shRNA were transformed into competent *E. coli* cells (Shanghai GeneChem Co., Ltd.) and transformed cells in serum-free LB solid medium (pH 7.0; Shanghai GeneChem Co., Ltd.) supplemented with ampicillin (0.1 mg/ml; Genebase) were cultured at 37˚C. Positive colonies were selected by reverse transcription-quantitative PCR (RT-qPCR) and sequencing. To construct a stable eIF3C-depletion cell line, cells were seeded in 6-well plates at a density of $5x10^4$ cells/well, grown overnight, and transfected with eIF3C-shRNA ($8x10^8$ TU/ml) (sheIF3C) or negative control shRNA ($1x10^9$ TU/ml) (shCtrl) lentivirus for 12 h. The culture medium was subsequently replaced with fresh complete RPMI-1640 medium, and cells were grown for an additional 72 h and subjected to fluorescence microscopy for the visualization of the green fluorescence protein (GFP). The efficiency of eIF3C depletion was evaluated through RT-qPCR and western blotting.

RT-qPCR. Total cellular RNA was isolated from ACHN, 786-O, A498 and Caki-1 cell lines using TRIzol® reagent (Shanghai Pufei Biotechnology Co., Ltd.) and reverse transcribed into cDNA using the M-MLV cDNA kit (Promega Corporation) according to the manufacturer's instructions. The following steps were used: Step 1, adding 2 μg total RNA, 1 μl Oligo(dT) and RNase-Free H_2O to 10 μl total volume, heating at 70˚C for 5 sec; step 2, adding 4 μl 5X RT buffer, 2 μl 10 m MdNTPs, 0.4 μl Rnasin (40 U/μl), 1 μl M-MLV-RTase (200 U/μl) and 2.6 μl RNase-Free H_2O, heating at 42˚C for 1 h and at 70˚C for 10 min. Real-time quantitative polymerase chain reaction (RT-qPCR) was performed to assess the expression levels of eIF3C using a SYBR Master Mixture kit (cat. no. DRR041B)

from Takara Biotechnology Co., Ltd. according to the manufacturer's instructions. The following thermocycling conditions were used: Stage 1, holding at 95˚C for 30 sec, 1 cycle; stage 2, 2 steps PCR reacting at 95˚C for 5 sec and at 60˚C for 30 sec, respectively, 45 cycles; stage 3, dissociating at 95˚C for 15 sec, at 55˚C for 30 sec and at 95˚C for 15 sec, respectively, 1 cycle. GAPDH was used as an internal control. The primers were designed as follows: Human eIF3C forward, 5'-AGATGAGGA TGAGGATGAGGAC-3' and reverse, 5'-GGAATCGGAAGA TGTGGAACC-3'; and human GAPDH forward, 5'-TGACTT CAACAGCGACACCCA-3' and reverse, 5'-CACCCTGTT GCTGTAGCCAAA-3'. The relative expression level of eIF3C was calculated using the $2^{-\Delta\Delta Cq}$ method (30). The experiments were performed in triplicate.

Celigo cell viability and proliferation assay. Following depletion of elF3c expression, tumor cells were subjected to a cell proliferation assay. Briefly, after 24 h gene transfection, ACHN cells were seeded into 96-well plates at a density of $2x10^3$ cells/well and grown for up to 5 days. On each day, the green fluorescence emission was observed and recorded using a Celigo cytometer (Nexcelom Bioscience) to assess the proliferation of tumor cells. The data are presented as the mean ± SD (n=3).

The 96-well plates were subjected to an MTT assay using the MTT reagent (Genview) and formazan was dissolved by DMSO solution (Shiyi Corporation). An ELIASA microplate reader (Tecan Group, Ltd.) was used and the optical density value at 490 nm was used to estimate cell confluence. The data are presented as the mean ± SD (n=3).

Cell cycle distribution assay. ACHN cells were cultured in 6-cm cell culture dishes until they reached 80% confluence, and were then transfected for 5 days with a lentivirus targeting eIF3C or a negative control shRNA. Cells were then harvested, washed with ice-cold D-Hanks solution, and fixed with 75% ethyl alcohol at 4˚C for at least 1 h. Subsequently, cells were washed with ice-cold D-Hanks solution and stained with 40X propidium iodide solution (2 mg/ml), 100X RNase (10 mg/ml) and 1X D-Hanks solution according to the manufacturer's instructions (Sigma-Aldrich; Merck KGaA). The cell cycle distributions were then analyzed using Guava easyCyte HT flow cytometry (EMD Millipore) and the results were analyzed by ModFit LT 4.0 software (Verity Software House, Inc.).

Cell apoptosis assay. ACHN cells were cultured in 6-cm cell culture dishes until they reached 80% confluence, and were transfected for 5 days with a lentivirus targeting eIF3C or a negative control shRNA. Transfected cells were harvested, washed with ice-cold D-Hanks solution and fixed with 75% ethyl alcohol at 4˚C for at least 1 h. Staining was performed using Annexin V-APC apoptosis detection kit (eBioscience; Thermo Fisher Scientific, Inc.) according to the manufacturer's instructions. Briefly, the cells were collected by centrifugation at 265 x g at 4˚C for 5 min, washed with D-Hanks solution and then mixed with 1X binding buffer. Subsequently, 200 μl cell suspension was thoroughly mixed with 10 μl Annexin V solution, followed by incubation in the dark at room temperature for 10-15 min. Cells were then subjected to Guava easyCyte HT flow cytometry (EMD Millipore) and the results were analyzed by ModFit LT 4.0 software (Verity Software House, Inc.).

Nude mouse tumor xenograft formation assay. The animal protocol was approved by the Institutional Animal Care and Use Committee of the Third Affiliated Hospital of Soochow University (Changzhou, China). Female BALB/c nude mice (n=14; 4 weeks old; average weight, 18.7±1.75 g) were obtained from Shanghai SLAC Laboratory Animal Co., Ltd. All mice were raised under specific pathogen-free conditions (23±3˚C; relative humidity, 40-70%) under a 12 h light/dark cycle. All mice were adaptively fed with free access to water and standard mouse chow. Animals were randomly divided into two experimental groups and subcutaneously injected into the right forelimb armpit with $1x10^7$ 786-O cells (in ~200 μl PBS) following transfection with a lentivirus carrying eIF3C- or scrambled shRNA. Mice were regularly monitored for weight, health and xenograft size for 7 weeks. Subsequently, all mice were euthanized by injection of 2% sodium pentobarbital (150 mg/kg of body weight), and after complete coma, cervical dislocation was performed. The tumor volume was measured for the greatest longitudinal diameter (length) and the greatest transverse diameter (width) using a vernier caliper. The tumor volume was calculated using the modified ellipsoidal formula as follows: $V=3.14/6 \times L \times W^2$, in which V represents the whole volume of the tumor cell xenograft (mm^3), L indicates the length (mm), and W is the width (mm).

Microarray and ingenuity pathway analyses. Total cellular RNA was isolated from 786-O cells after transfection with a lentivirus carrying eIF3C-shRNA (n=3) or scrambled shRNA (n=3) using TRIzol® reagent (31). RNA quantity and quality were evaluated using a NanoDrop 2000 spectrophotometer (Thermo Fisher Scientific, Inc.) and RNA 2100 (Agilent Technologies, Inc.), respectively, according to the manufacturers' instructions. The genome-wide effects of eIF3C depletion were evaluated by GeneChip PrimeView Human Affymetrix microarray (Affymetrix; Thermo Fisher Scientific, Inc.) according to the manufacturer's instructions. The resultant raw data and the differentially expressed genes (DEGs) in the eIF3C-shRNA-infected RCC cell lines were identified based on the criteria of an absolute fold change >1.3 and P<0.05. An ingenuity pathway analysis (Ingenuity Systems; Qiagen, Inc.) was performed to assess the functional and pathway annotations based on all the DEGs.

Western blotting. Total cellular protein from tissue samples and cell lines was extracted using an ice-cold RIPA (high) lysis buffer (Beyotime Institute of Biotechnology) and centrifuged at 12,000 x g at 4˚C for 15 min. The protein concentration was determined using the bicinchoninic acid protein assay kit (Beyotime Institute of Biotechnology). Equal amounts of protein (30 μg/μl) were separated by 10% SDS-PAGE and then transferred onto PVDF membranes (EMD Millipore). These membranes were blocked with 5% fat-free milk in TBS-0.5% Tween-20 (TBS-T) at room temperature for 1 h and then incubated with primary antibodies at room temperature for 2 h. The antibodies used in the present study were anti-c-JUN (1:200 dilution; cat. no. ab32137; Abcam), anti-NFKB inhibitor α (NFKBIA; 1:2,000 dilution; cat. no. ab7217;

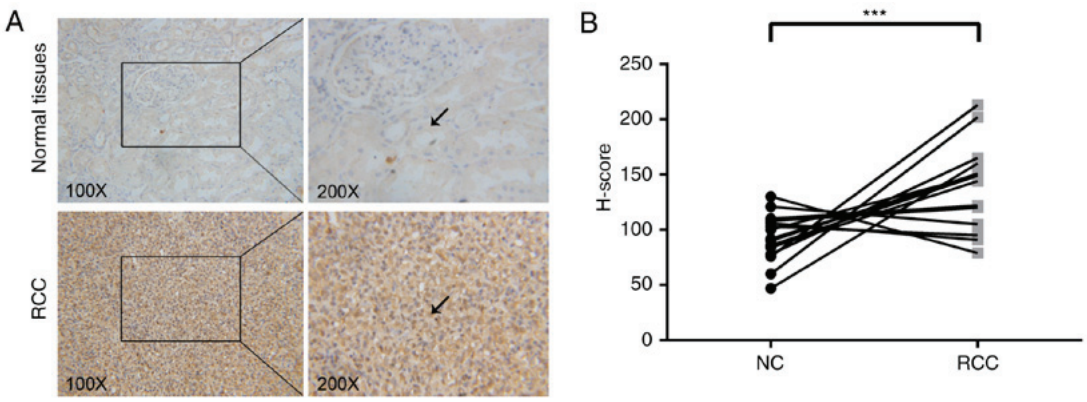

Figure 1. eIF3C is upregulated in RCC tissues. (A) Immunohistochemistry. The RCC tissues and their distant normal tissues were cut into 4-μM thick sections and subjected to immunohistochemical analysis of eIF3C expression. (B) H-scores of 16 individual cases. Following immunostaining of eIF3C protein in RCC tissues, H-scores were calculated. ***P<0.001, as indicated. eIF3C, eukaryotic initiation factor 3c; NC, negative control; RCC, renal cell carcinoma.

Abcam), anti-AKT (1:1,000 dilution; cat. no. 9272; Cell Signaling Technology, Inc.), anti-phosphorylated-(p-)AKT (1:1,000 dilution; cat. no. 13038; Cell Signaling Technology, Inc.), anti-caspase-3 (1:1,000 dilution; cat. no. 9662; Cell Signaling Technology, Inc.), anti-caspase-8 (1:1,000 dilution; cat. no. 4790; Cell Signaling Technology, Inc.), anti-caspase-9 (1:1,000 dilution; cat. no. ab2324; Abcam) and anti-GAPDH (1:2,000 dilution; cat. no. sc-32233; Santa Cruz Biotechnology, Inc.). All aforementioned antibodies of caspases could detect both the cleaved and total caspases. Blots were washed three times in TBS-T and further incubated with a secondary antibody goat anti-mouse immunoglobulin G (IgG)-HRP (1:5,000 dilution; cat. no. sc-2005; Santa Cruz Biotechnology, Inc.) or goat anti-rabbit IgG-HRP (1:5,000 dilution; cat. no. sc-2004; Santa Cruz Biotechnology, Inc.) at room temperature for 90 min. Immunoreactive protein bands were developed using the Pierce™ ECL Western Blotting Substrate kit (Thermo Fisher Scientific, Inc.) and exposed to x-ray films. The protein bands were semi-quantified using ImageJ v1.37 software (National Institutes of Health).

Statistical analysis. All data are presented as the mean ± SD of at least three repeated experiments, and the difference between groups was analyzed using Student's t-test by GraphPad Prism v6.0 software (GraphPad Software, Inc.). P<0.05 was considered to indicate a statistically significant difference.

Results

eIF3C expression is upregulated in RCC tissues. The present study analyzed the expression levels of eIF3C in 16 paired RCC and distant normal tissues using immunohistochemistry. In almost all cases, eIF3C staining was stronger in the RCC tissue compared with in the paired distant normal tissue (Fig. 1A). Subsequently, the immunostaining data was quantified using the H-score. The H-score was significantly higher in the RCC tissue compared with in the normal tissues (Fig. 1B), indicating that eIF3C may contribute to the development or progression of RCC.

RCC cell proliferation is reduced and cell cycle distribution is altered following eIF3C depletion. The present study assessed the mRNA expression levels of eIF3C in four different RCC cell lines using RT-qPCR. eIF3C expression was high in all four tested cell lines (Fig. 2F). Among them, eIF3C mRNA exhibited the highest expression levels in 786-O cells and the lowest expression levels in ACHN cells. Therefore, ACHN and 786-O cell lines were selected for subsequent experiments in which eIF3C was depleted (Fig. 2A), and alterations in the tumor cell malignant phenotypes were explored. Fig. 2G-I shows that transfection with a lentivirus carrying eIF3C-shRNA resulted in significantly decreased eIF3C mRNA and protein expression compared with transfection with lentivirus carrying shCtrl.

Subsequently, the proliferation capacity of these tumor cells was assessed using cell proliferation and viability assays. The present study revealed that depletion of eIF3C significantly reduced the viability and proliferation rate of ACHN and 786-O cells compared with the control group (Fig. 2B-E). Additionally, the depletion of eIF3C remarkably altered the cell cycle distribution. There were 42.64±0.81, 53.70±1.28 and 3.67±0.60% of tumor cells in G_1, S and G_2 phases, respectively, following transfection with shCtrl, whereas there were 49.64±0.77, 45.96±0.46 and 4.40±0.41% of tumor cells in G_1, S and G_2 phases, respectively, after transfection with eIF3C-shRNA (Fig. 3A and B). The number of G_1-phase cells was significantly higher in the sheIF3C group compared with in the shCtrl group (P<0.001). However, the numbers of S-phase cells were lower in the sheIF3C group compared with in the shCtrl group (P<0.001).

Depletion of eIF3C triggers apoptosis of RCC cells. To assess the underlying mechanism of the reduced cell viability following the depletion of eIF3C, an apoptosis assay by flow cytometry as performed. The proportion of apoptotic cells in eIF3C-depleted ACHN cells was ~2-fold higher compared with in the cells transfected with scrambled shRNA (7.57±0.38 vs. 3.73±0.16%, P<0.01; Fig. 3C and D). Additionally, the expression levels of caspase-3, caspase-8 and caspase-9 were detected, and it was ascertained that the depletion of eIF3C could induce their upregulation with the exception of caspase-8 (Fig. 3E and F).

Effects of reduced eIF3C expression on the formation and growth of nude mouse xenograft. The *in vitro* findings were

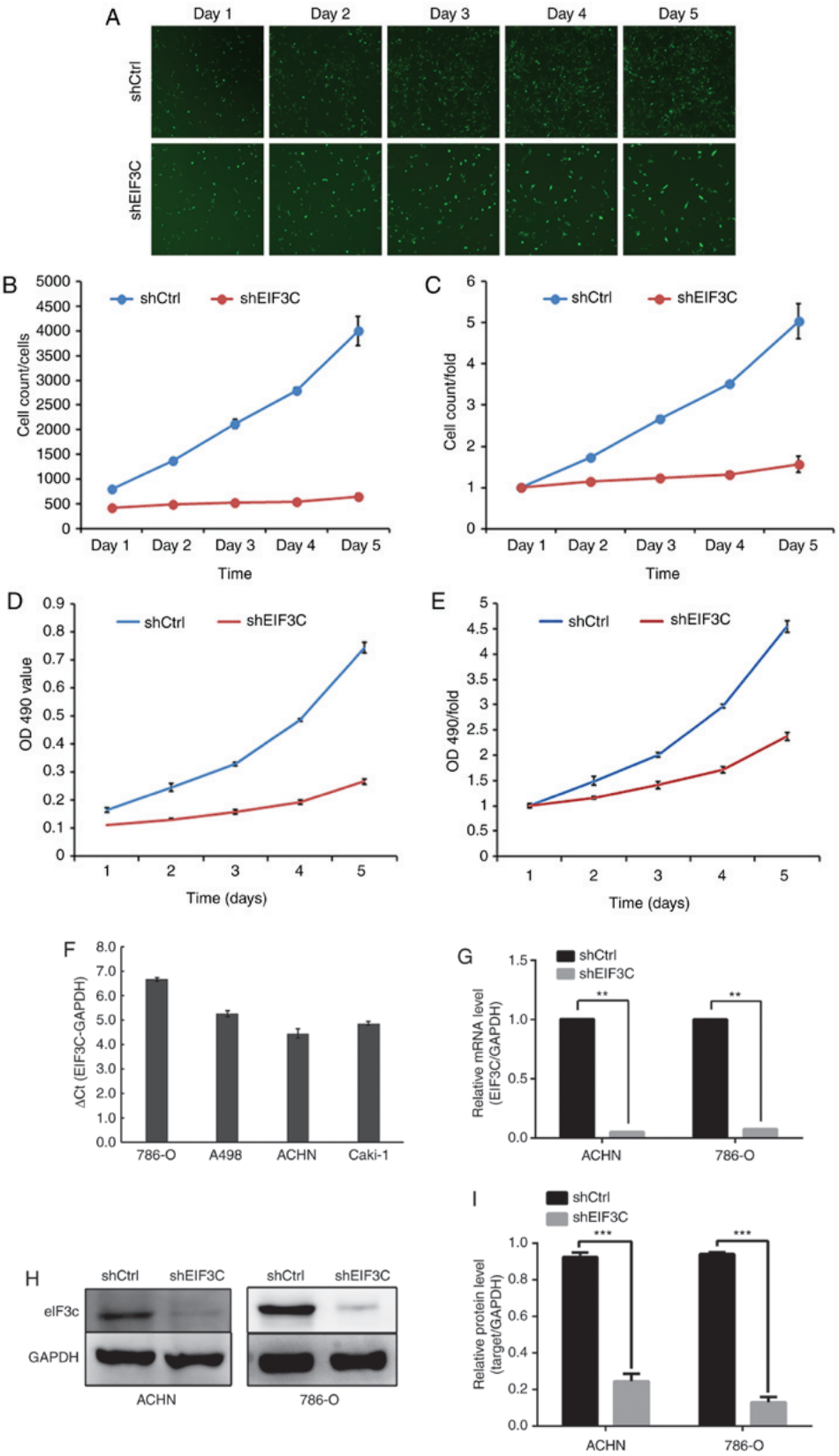

Figure 2. eIF3C facilitates the proliferation of renal cell carcinoma cells *in vitro*. (A) Fluorescence microscopy. The images were captured once a day following transfection with a lentivirus carrying sheIF3C or shCtrl in ACHN cells. Magnification, x15. (B) Cell proliferation Celigo assay. The cells were cultured and transfected with a lentivirus carrying sheIF3C or shCtrl for up to 5 days and the number of cells was counted. (C) Cell proliferation Celigo assay. The fold of cell growth was assessed. (D) Cell viability MTT assay. The cells were cultured and transfected with a lentivirus carrying sheIF3C or shCtrl for up to 5 days and the OD490 value was examined. (E) Cell viability MTT assay. The fold of OD490 value was obtained. (F) RT-qPCR. The cells were cultured and subjected to RT-qPCR. GAPDH was used as an internal control. (G) RT-qPCR. The cells were cultured and transfected with a lentivirus carrying sheIF3C or shCtrl for 72 h and subjected to RT-qPCR. $^{**}P<0.01$, as indicated. (H) Western blotting. The cells were cultured and transfected with a lentivirus carrying sheIF3C or shCtrl for 72 h and subjected to western blotting. (I) Semi-quantified data from blots shown in (H) using densitometric analysis (ImageJ software). $^{***}P<0.001$, as indicated. eIF3C, eukaryotic initiation factor 3c; sheIF3C, GFP-eIF3C-shRNA; shCtrl, GFP-scrambled-shRNA; RT-qPCR, reverse transcription-quantitative PCR; OD, optical density.

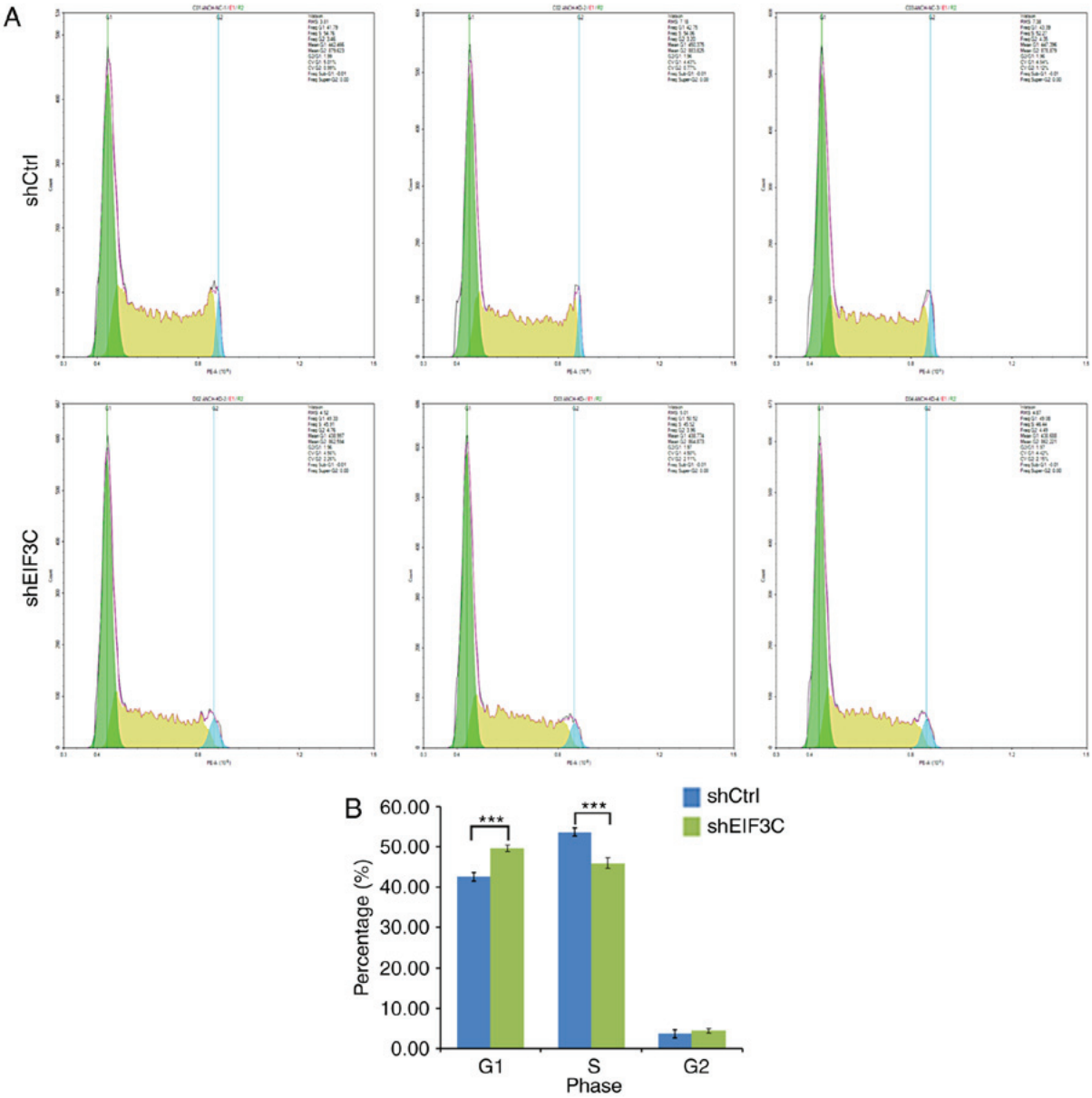

Figure 3. eIF3C depletion induces cell cycle arrest and apoptosis of renal cell carcinoma cells *in vitro*. (A) Flow cytometric cell cycle distribution assay. The cells were cultured and transfected with a lentivirus carrying sheIF3C or shCtrl for 5 days and subjected to a flow cytometric cell cycle distribution assay. (B) Summarized data from the cell cycle distribution assay. **P<0.01 and ***P<0.001, as indicated. eIF3C, eukaryotic initiation factor 3c; sheIF3C, GFP-eIF3C-shRNA; shCtrl, GFP-scrambled-shRNA.

further confirmed using a nude mouse tumor cell xenograft assay. At the beginning of the experiment, the average weights of the sheIF3C and shCtrl mice were 18.5±2.32 and 18.9±0.99 g, respectively. At the end of the experiment, the average body weights of the sheIF3C and shCtrl mice were 22.9±2.30 and 23.0±0.96 g, respectively (data not shown). The average tumor volume of the sheIF3C group was 106.72 mm^3, whereas it was 491.61 mm^3 in the shCtrl group (Fig. 4). Additionally, the average tumor xenograft weight in the sheIF3C group was significantly lower compared with the shCtrl group (0.100±0.10 vs. 0.45±0.132 g; P<0.05; Fig. 4).

Effects of reduced eIF3C expression on gene expression in vitro and in vivo. To explore the potential molecular events following eIF3C depletion, a microarray analysis was conducted to identify DEGs in eIF3C-depleted RCC 786-O cells. A total of 994 DEGs were identified, including 516 upregulated and 478 downregulated genes (Fig. 5A). The ingenuity pathway analysis revealed that eIF3C-regulated genes were mainly involved in the pathways of 'cell growth and proliferation', 'cell death and survival', 'cancer', 'organismal injury and abnormalities', 'cell cycle', 'cellular development' and 'cellular movement' (Fig. 5B). Common tumor-associated genes, such as AKT, c-JUN and NFKBIA, whose expression levels changed significantly, were selected. Western blotting results revealed that all of them could be regulated by eIF3C (Fig. 5C and D).

Discussion

RCC is usually diagnosed at advanced stages of the disease and is insensitive to chemoradiotherapy (5). Therefore, identification of novel gene alterations and targets involved in this

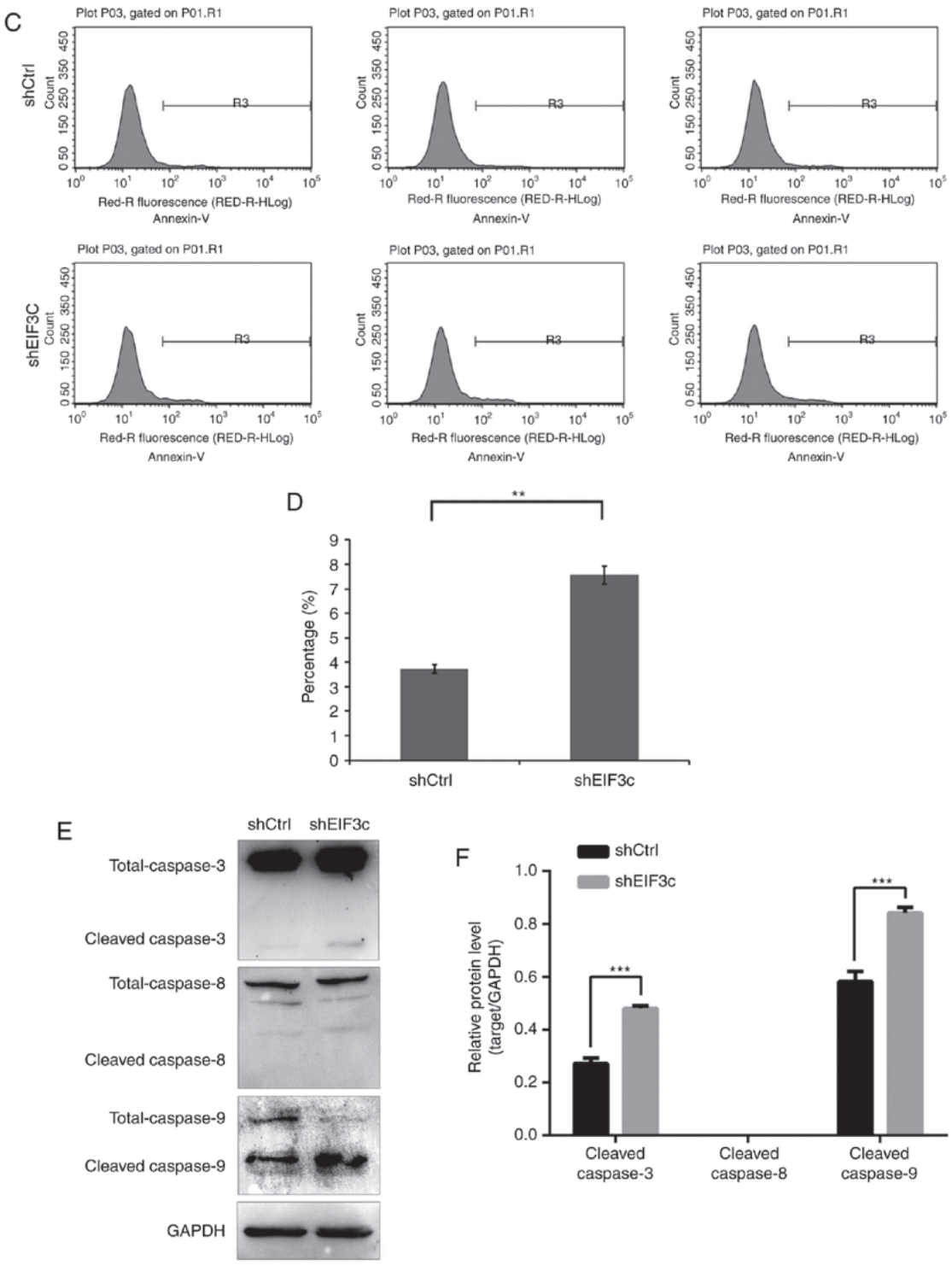

Figure 3. Continued. (C) Flow cytometric apoptosis assay. The cells were cultured and transfected with a lentivirus carrying sheIF3C or shCtrl for 5 days and subjected to a flow cytometric cell apoptosis assay. (D) Summarized data from the apoptosis assay. (E) Western blotting. The ACHN cells were cultured and transfected with a lentivirus carrying sheIF3C or shCtrl for 5 days and subjected to estern blot analysis. (F) Semi-quantified data from (E) using densitometric analysis (ImageJ software). **P<0.01 and ***P<0.001, as indicated. eIF3C, eukaryotic initiation factor 3c; sheIF3C, GFP-eIF3C-shRNA; shCtrl, GFP-scrambled-shRNA.

disease could help medical oncologists effectively control RCC in clinical practice. The present study first assessed eIF3C expression at the protein level in RCC and normal kidney tissues and then investigated the effects of eIF3C depletion on the regulation of malignant behaviors of RCC cells *in vitro* and in nude mice. The data revealed that eIF3C protein expression was significantly higher in RCC tissues and cell lines compared with their corresponding controls. The depletion of eIF3C reduced tumor cell proliferation, increased the proportion of G_1-phase tumor cells, and enhanced tumor cell apoptosis compared with the controls. Furthermore, depletion of eIF3C also inhibited the formation and growth of tumor cell xenograft in nude mice. At the gene level, depletion of eIF3C resulted in 516 upregulated and 478 downregulated

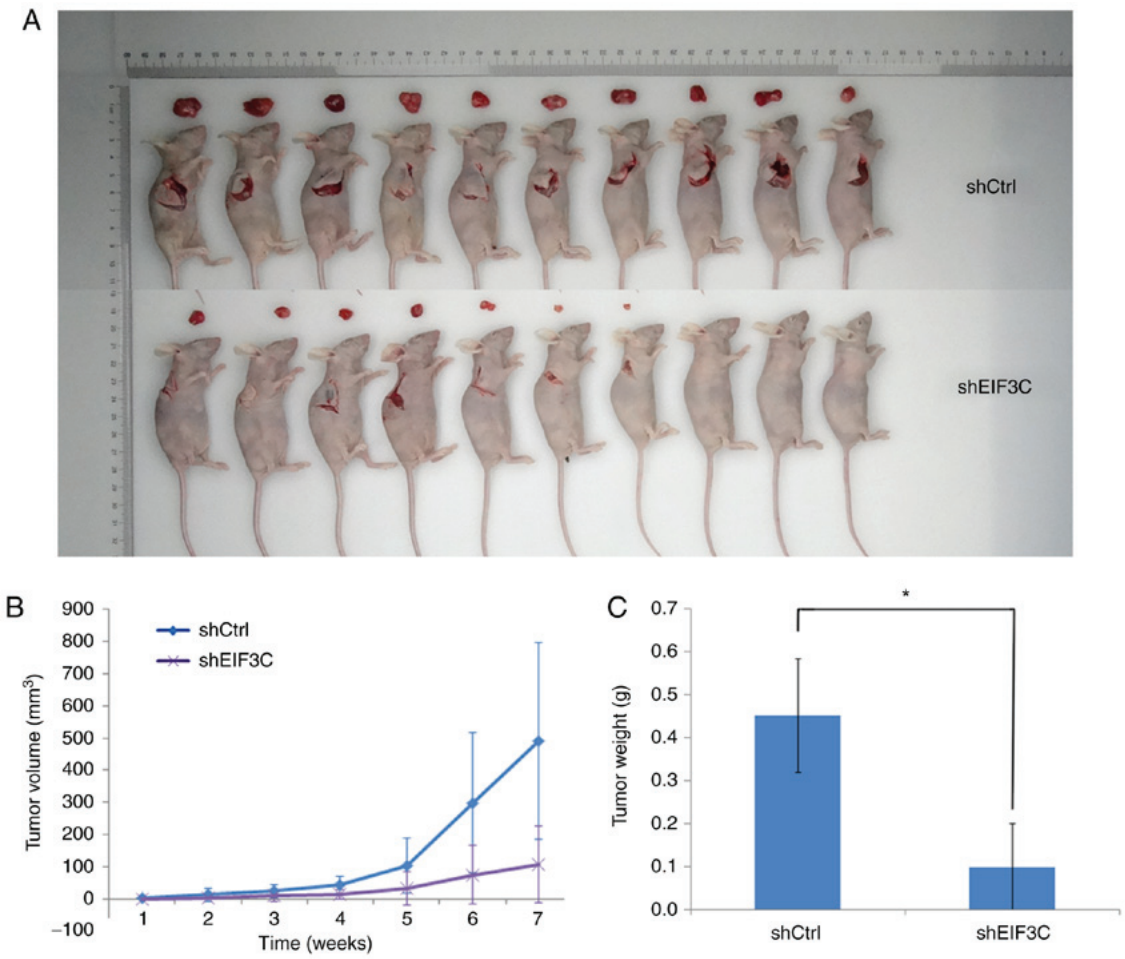

Figure 4. eIF3C depletion inhibits the formation and growth of xenografts *in vivo*. (A) renal cell carcinoma 786-O cells were transfected with a lentivirus carrying sheIF3C or shCtrl. These cells were then subcutaneously injected into the nude mice (n=10 per group) and mice were monitored for 7 weeks. (B) Tumor volume was monitored and recorded once a week. (C) Tumor weights were measured after 7 weeks. *P<0.05, as indicated. eIF3C, eukaryotic initiation factor 3c; sheIF3C, GFP-eIF3C-shRNA; shCtrl, GFP-scrambled-shRNA.

genes. These genes were involved in cell proliferation, survival and cancer-related pathways, including the AKT, c-JUN and NFKBIA signaling pathways. These findings were confirmed through western blotting. Collectively, the data demonstrated that eIF3C exerted oncogenic effects on the development and progression of RCC.

The proteins in the eIF family mainly function as initiators of protein translation from their corresponding mRNAs in eukaryotic cells (32). To date, ~11 eIF members have been reported to be involved in this process (16). One of these protein family members, eIF3, has 13 different subunits (eIF3a to eIF3 m) (16) that can bind to the 40S ribosome through the facilitation of methionyl-tRNA and mRNA binding for protein translation (33). Previous studies have demonstrated that the eIF3C subunit of eIF3 is a crucial binding partner for eIF1 and eIF5 (34,35), and this subunit serves an essential role in the selection of the translational start codon (36). During the development and progression of cancer, protein synthesis is frequently upregulated, and overexpression of eIF3C has been observed in various types of cancer (19-26). However, to the best of our knowledge, no studies have investigated the role of eIF3C in RCC. The present study demonstrated that eIF3C expression was upregulated in RCC tissues and cell lines. Zang *et al* (37) have reported that overexpression of eIF3b in tumors is associated with an aggressive tumor phenotype and poor prognosis in patients with RCC. However, as the present study had a small sample size, future studies with large tissue sample sizes can further confirm the upregulation of eIF3C and determine whether such upregulation is associated with the prognosis or even the treatment response in RCC.

The data revealed that depletion of eIF3C inhibited the malignant behavior in RCC, including a decrease in tumor cell proliferation, increased apoptosis and altered cell cycle progression. This corroborates the important role of eIF3C in the development and progression of RCC. Indeed, a previous study has demonstrated that eIF3C is able to induce exosome secretion and promote angiogenesis and tumorigenesis in human hepatocellular carcinoma (25). In breast cancer, eIF3C targets the mTOR signaling pathway to inhibit cell proliferation and induce apoptosis (26). Therefore, targeting eIF3C could be a potential therapeutic approach for cancer treatment (13). Furthermore, the expression of other eIF3 subunits could also be altered in RCC. For example, aberrant eIF3e expression is essential for embryonic development and cell proliferation (38), whereas aberrant eIF3a expression occurs in non-small cell lung cancer, which is associated with p27 expression and poor patient prognosis (39). Additionally, eIF3b is able to activate the β-catenin signaling pathway, leading to accelerated progression

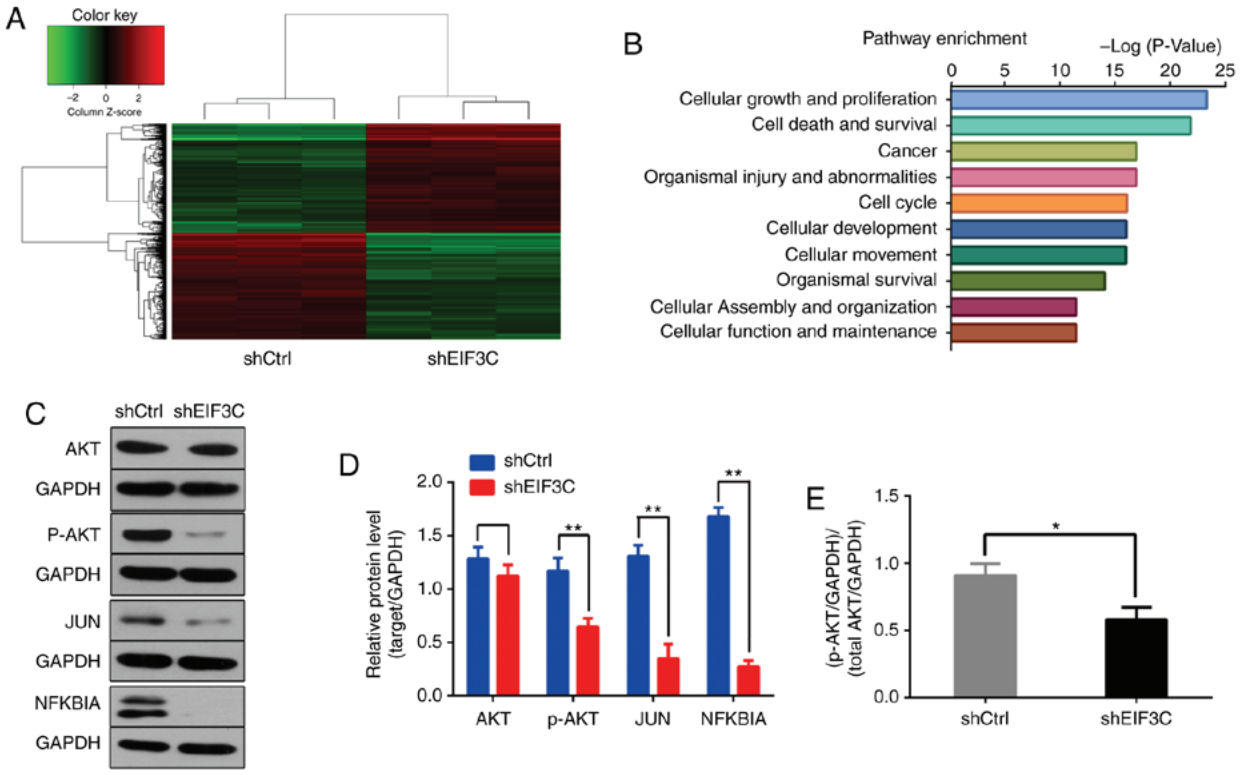

Figure 5. Effects of eIF3C depletion on the regulation of gene expression. (A) Hierarchical clusters of DEGs were analyzed using the Affymetrix microarray. (B) Functional and pathway annotations of DEGs in eIF3C-depleted 786-O cells vs. the negative control. (C) Western blotting. The 786-O cells were cultured and transfected with a lentivirus carrying eIF3C-shRNA (sheIF3C) or scrambled shRNA (shCtrl) for 48 h and subjected to Western blotting analysis. (D) Semi-quantified data from (C) using densitometric analysis (ImageJ software). (E) Changes in the ratio of p-AKT to total AKT in the two groups from (D). *P<0.05, **P<0.01, as indicated. Ctrl, control; DEGs, differentially expressed genes; eIF3C, eukaryotic initiation factor 3c; NFKBIA, NFKB inhibitor α; P-, phosphorylated-; sh, short hairpin RNA.

of esophageal squamous cell carcinoma (40). Zhu *et al* (41) have reported that eIF3 h targets the transforming growth factor-β and mitogen-activated protein kinase signaling pathways in patients with hepatocellular carcinoma. Qi *et al* (42) have reported that overexpression of eIF3i can activate the synthesis of prostaglandin-endoperoxide synthase 2 and β-catenin in colorectal cancer. Therefore, it is necessary to further investigate the functions of eIF3C in the development and progression of RCC.

In the present study, it was also observed that depletion of eIF3C was able to suppress different signaling pathways, including the Akt, c-JUN and NFKBIA singaling pathways. This indicated that eIF3C promoted RCC malignant phenotypes *in vitro* through these signaling pathways. Several eIFs family members have been found to participate in these pathways indicated above in various tumors, such as lung cancer, breast cancer, hepatocellular cancer and intestinal cancer (17). A previous study has linked eIF1, eIF5 and eIF6 to the PI3K/Akt/mTOR signaling pathway in colorectal cancer (43), whereas Zang *et al* (37) has demonstrated that depletion of eIF3b suppresses the Akt pathway network in RCC cells, including decreased expression of integrin/focal adhesion kinase/Akt,Akt/mTOR/hypoxia-inducible factor/vascular endothelial growth factor, Akt/mTOR/NF-κB, Akt/Bcl-2/Bax and Akt/glycogen synthase kinase-3β pathway genes. Furthermore, Chen *et al* (44) have demonstrated that eIF4b may integrate the signals from the Pim and PI3K/Akt/mTOR signaling pathways in Abl-expressing leukemic cells. Phosphorylated eIF2 exhibits translation-dependent control of the activation of NF-κB (45). In order to review what occurred in tumors, the aforementioned signaling pathways were listed in Table SI. However, there was insufficient data demonstrating eIF3C-related gene regulation. The present study demonstrated that there were a total of 994 differentially expressed genes in RCC cells following eIF3C depletion. Future studies could characterize some of these genes in RCC cells.

Overall, the findings provided initial evidence regarding the role of eIF3C in the development and progression of RCC. However, the underlying molecular mechanisms require further investigation.

Acknowledgements

Not applicable.

Funding

The present study was financially supported in part by grants from the Natural Science Foundation of Jiangsu Province (grant no. BK20151180), Applied Basic Research of Changzhou City (grant no. CJ20159014) and Major Science and Technology Project of Changzhou Health Bureau (grant no. ZD201405).

Availability of data and materials

The datasets used and/or analyzed during the current study are available from the corresponding author on reasonable request.

Authors' contributions

XH and ZC conceived and designed the project. KW, HY and XW performed the experiments and acquired the data. MF analyzed the data. KW and MF participated in writing the article. All authors read and approved the final version of this manuscript.

Ethics approval and consent to participate

Written informed consent was obtained from every participant enrolled in the present study. The current study was approved by the Ethics Committee of the Third Affliated Hospital of Soochow University.

Patient consent for publication

All patients in the present study provided consent for their data to be published.

Competing interests

The authors declare that they have no competing interests.

References

1. Birkhäuser FD, Kroeger N and Pantuck AJ: Etiology of renal cell carcinoma: Incidence, demographics, and environmental factors. In: Renal Cell Carcinoma: Clinical Management. Springer Science, New York, NY, pp3-22, 2013.
2. Zhou M and He H: Pathology of renal cell carcinoma. Renal Cancer 43: 51-69, 2013.
3. Gupta K, Miller JD, Li JZ, Russell MW and Charbonneau C: Epidemiologic and socioeconomic burden of metastatic renal cell carcinoma (mRCC): A literature review. Cancer Treat Rev 34: 193-205, 2008.
4. Cohen HT and McGovern FJ: Renal-cell carcinoma. N Engl J Med 353: 2477-2490, 2005.
5. Najjar YG and Rini BI: Novel agents in renal carcinoma: A reality check. Ther Adv Med Oncol 4: 183-194, 2012.
6. Rini BI, Campbell SC and Escudier B: Renal cell carcinoma. Lancet 373: 1119-1132, 2009.
7. Rohan SM, Xiao Y, Liang Y, Dudas ME, Al-Ahmadie HA, Fine SW, Gopalan A, Reuter VE, Rosenblum MK, Russo P and Tickoo SK: Clear-cell papillary renal cell carcinoma: Molecular and immunohistochemical analysis with emphasis on the von Hippel-Lindau gene and hypoxia-inducible factor pathway-related proteins. Mod Pathol 24: 1207-1220, 2011.
8. Wu CZ, Zheng JJ, Bai YH, Xia P, Zhang HC and Guo Y: HMGB1/RAGE axis mediates the apoptosis, invasion, autophagy, and angiogenesis of the renal cell carcinoma. Onco Targets Ther 11: 4501-4510, 2018.
9. Zhai W, Ma J, Zhu R, Xu C, Zhang J, Chen Y, Chen Z, Gong D, Zheng J, Chen C, *et al*: MiR-532-5p suppresses renal cancer cell proliferation by disrupting the ETS1-mediated positive feedback loop with the KRAS-NAP1L1/P-ERK axis. Br J Cancer 119: 591-604, 2018.
10. Damayanti NP, Budka JA, Khella HWZ, Ferris MW, Ku SY, Kauffman E, Wood AC, Ahmed K, Chintala VN, Adelaiye-Ogala R, *et al*: Therapeutic targeting of TFE3/IRS-1/PI3K/mTOR axis in translocation renal cell carcinoma. Clin Cancer Res 24: 5977-5989, 2018.
11. Carlo MI, Mukherjee S, Mandelker D, Vijai J, Kemel Y, Zhang L, Knezevic A, Patil S, Ceyhan-Birsoy O, Huang KC, *et al*: Prevalence of germline mutations in cancer susceptibility genes in patients with advanced renal cell carcinoma. JAMA Oncol 4: 1228-1235, 2018.
12. Mitchell TJ, Rossi SH, Klatte T and Stewart GD: Genomics and clinical correlates of renal cell carcinoma. World J Urol 36: 1899-1911, 2018.
13. Emmanuel R, Weinstein S, Landesman-Milo D and Peer D: eIF3c: A potential therapeutic target for cancer. Cancer Lett 336: 158-166, 2013.
14. Sonenberg N and Hinnebusch AG: Regulation of translation initiation in eukaryotes: Mechanisms and biological targets. Cell 136: 731-745, 2009.
15. Zhou M, Sandercock AM, Fraser CS, Ridlova G, Stephens E, Schenauer MR, Yokoi-Fong T, Barsky D, Leary JA, Hershey JW, *et al*: Mass spectrometry reveals modularity and a complete subunit interaction map of the eukaryotic translation factor eIF3. Proc Natl Acad Sci USA 105: 18139-18144, 2008.
16. Hinnebusch AG: eIF3: A versatile scaffold for translation initiation complexes. Trends Biochem Sci 31: 553-562, 2006.
17. Hershey JW: The role of eIF3 and its individual subunits in cancer. Biochim Biophys Acta 1849: 792-800, 2015.
18. Bhat M, Robichaud N, Hulea L, Sonenberg N, Pelletier J and Topisirovic I: Targeting the translation machinery in cancer. Nat Rev Drug Discov 14: 261-278, 2015.
19. Rothe M, Ko Y, Albers P and Wernert N: Eukaryotic initiation factor 3 p110 mRNA is overexpressed in testicular seminomas. Am J Pathol 157: 1597-1604, 2000.
20. Scoles DR, Yong WH, Qin Y, Wawrowsky K and Pulst SM: Schwannomin inhibits tumorigenesis through direct interaction with the eukaryotic initiation factor subunit c (eIF3c). Hum Mol Genet 15: 1059-1070, 2006.
21. Hao J, Liang C and Jiao B: Eukaryotic translation initiation factor 3, subunit C is overexpressed and promotes cell proliferation in human glioma U-87 MG cells. Oncol Lett 9: 2525-2533, 2015.
22. Hao J, Wang Z, Wang Y, Liang Z, Zhang X, Zhao Z and Jiao B: Eukaryotic initiation factor 3C silencing inhibits cell proliferation and promotes apoptosis in human glioma. Oncol Rep 33: 2954-2962, 2015.
23. Song N, Wang Y, Gu XD, Chen ZY and Shi LB: Effect of siRNA-mediated knockdown of eIF3c gene on survival of colon cancer cells. J Zhejiang Univ Sci B 14: 451-459, 2013.
24. Li T, Li S, Chen D, Chen B, Yu T, Zhao F, Wang Q, Yao M, Huang S, Chen Z and He X: Transcriptomic analyses of RNA-binding proteins reveal eIF3c promotes cell proliferation in hepatocellular carcinoma. Cancer Sci 108: 877-885, 2017.
25. Lee HY, Chen CK, Ho CM, Lee SS, Chang CY, Chen KJ and Jou YS: eIF3C-enhanced exosome secretion promotes angiogenesis and tumorigenesis of human hepatocellular carcinoma. Oncotarget 9: 13193-13205, 2018.
26. Zhao W, Li X, Wang J, Wang C, Jia Y, Yuan S, Huang Y, Shi Y and Tong Z: Decreasing eukaryotic initiation factor 3C (eIF3C) suppresses proliferation and stimulates apoptosis in breast cancer cell lines through mammalian target of rapamycin (mTOR) pathway. Med Sci Monit 23: 4182-4191, 2017.
27. Hammes LS, Tekmal RR, Naud P, Edelweiss MI, Kirma N, Valente PT, Syrjänen KJ and Cunha-Filho JS: Up-regulation of VEGF, c-fms and COX-2 expression correlates with severity of cervical cancer precursor (CIN) lesions and invasive disease. Gynecol Oncol 110: 445-451, 2008.
28. ANSI/ATCC ASN-0002–2011. Authentication of Human Cell Lines: Standardization of STR Profiling. ANSI eStandards Store, 2012.
29. Capes-Davis A, Reid YA, Kline MC, Storts DR, Strauss E, Dirks WG, Drexler HG, MacLeod RA, Sykes G, Kohara A, *et al*: Match criteria for human cell line authentication: Where do we draw the line? Int J Cancer 132: 2510-2519, 2013.
30. Livak KJ and Schmittgen TD: Analysis of relative gene expression data using real-time quantitative PCR and the 2(-Delta Delta C(T)) method. Methods 25: 402-408, 2001.
31. Chomczynski P and Sacchi N: Single-step method of RNA isolation by acid guanidinium thiocyanate-phenol-chloroform extraction. Anal Biochem 162: 156-159, 1987.
32. Dong Z and Zhang JT: Initiation factor eIF3 and regulation of mRNA translation, cell growth, and cancer. Crit Rev Oncol Hematol 59: 169-180, 2006.
33. Asano K, Vornlocher HP, Richter-Cook NJ, Merrick WC, Hinnebusch AG and Hershey JW: Structure of cDNAs encoding human eukaryotic initiation factor 3 subunits. Possible roles in RNA binding and macromolecular assembly. J Biol Chem 272: 27042-27052, 1997.
34. Karásková M, Gunišová S, Herrmannová A, Wagner S, Munzarová V and Valášek L: Functional characterization of the role of the N-terminal domain of the c/Nip1 subunit of eukaryotic initiation factor 3 (eIF3) in AUG recognition. J Biol Chem 287: 28420-28434, 2012.
35. Erzberger JP, Stengel F, Pellarin R, Zhang S, Schaefer T, Aylett CHS, Cimermančič P, Boehringer D, Sali A, Aebersold R and Ban N: Molecular architecture of the 40SeIF1eIF3 translation initiation complex. Cell 158: 1123-1135, 2014.

36. Srivastava S, Verschoor A and Frank J: Eukaryotic initiation factor 3 does not prevent association through physical blockage of the ribosomal subunit-subunit interface. J Mol Biol 226: 301-304, 1992.
37. Zang Y, Zhang X, Yan L, Gu G, Li D, Zhang Y, Fang L, Fu S, Ren J and Xu Z: Eukaryotic translation initiation factor 3b is both a promising prognostic biomarker and a potential therapeutic target for patients with clear cell renal cell carcinoma. J Cancer 8: 3049-3061, 2017.
38. Sadato D, Ono T, Gotoh-Saito S, Kajiwara N, Nomura N, Ukaji M, Yang L, Sakimura K, Tajima Y, Oboki K and Shibasaki F: Eukaryotic translation initiation factor 3 (eIF3) subunit e is essential for embryonic development and cell proliferation. FEBS Open Bio 8: 1188-1201, 2018.
39. Shen J, Yin JY, Li XP, Liu ZQ, Wang Y, Chen J, Qu J, Xu XJ, McLeod HL, He YJ, *et al*: The prognostic value of altered eIF3a and its association with p27 in non-small cell lung cancers. PLoS One 9: e96008, 2014.
40. Xu F, Xu CZ, Gu J, Liu X, Liu R, Huang E, Yuan Y, Zhao G, Jiang J, Xu C, *et al*: Eukaryotic translation initiation factor 3B accelerates the progression of esophageal squamous cell carcinoma by activating β-catenin signaling pathway. Oncotarget 7: 43401-43411, 2016.
41. Zhu Q, Qiao GL, Zeng XC, Li Y, Yan JJ, Duan R and Du ZY: Elevated expression of eukaryotic translation initiation factor 3H is associated with proliferation, invasion and tumorigenicity in human hepatocellular carcinoma. Oncotarget 7: 49888-49901, 2016.
42. Qi J, Dong Z, Liu J and Zhang JT: EIF3i promotes colon oncogenesis by regulating COX-2 protein synthesis and β-catenin activation. Oncogene 33: 4156-4163, 2014.
43. Golob-Schwarzl N, Schweiger C, Koller C, Krassnig S, Gogg-Kamerer M, Gantenbein N, Toeglhofer AM, Wodlej C, Bergler H, Pertschy B, *et al*: Separation of low and high grade colon and rectum carcinoma by eukaryotic translation initiation factors 1, 5 and 6. Oncotarget 8: 101224-101243, 2017.
44. Chen K, Yang J, Li J, Wang X, Chen Y, Huang S and Chen JL: eIF4B is a convergent target and critical effector of oncogenic Pim and PI3K/Akt/mTOR signaling pathways in Abl transformants. Oncotarget 7: 10073-10089, 2016.
45. Deng J, Lu PD, Zhang Y, Scheuner D, Kaufman RJ, Sonenberg N, Harding HP and Ron D: Translational repression mediates activation of nuclear factor kappa B by phosphorylated translation initiation factor 2. Mol Cell Biol 24: 10161-10168, 2004.